Proceedings of the 21st ICSMGE, Vienna, Austria, 14 – 19 June 2026. Pistrol, Adam & Schweiger (eds.)
Published by: ÖGG, Austrian Society for Geomechanics, Salzburg, Austria, ISBN 978-3-9503898-4-5
https://doi.org/10.53243/ICSMGE2026-987

Soil Nail Design for Surficial Slope Stabilization Using Flexible Facing Systems

Roman Gallus, Jean-Baptiste Payeur, Katharina Schwarz-Platzer, Lucie Sarthre, Theo Labourbe
Institute for Infrastructure and Environment, Bern University of Applied Science, roman.gallus@bfh.ch

Armin Roduner, Eberhard Gröner, Helene Lanter
Geobrugg AG

ABSTRACT: Flexible facing systems using steel wire mesh in combination with systematic nailing have proven to be highly effective for stabilizing slopes at the risk of failure in both soil and rock. Such systems have gained widespread acceptance due to their environmental and aesthetic advantages over shotcrete. This paper proposes a novel analytical design method particularly suited for flexible nails used for surficial slope stabilization. In contrast to existing design methods, the proposed approach treats the nails exclusively as tension members, thereby enabling a more efficient design. The paper further presents unique large-scale field tests enabling the physical simulation of slope instability and the assessment of the impact of flexible facing and nailing within a 10 m × 12 m test frame. Monitoring conducted during these tests provides valuable insights into the structural behavior and failure mechanisms of the slope stabilization system. The proposed design method is validated using force measurements obtained from the full-scale field tests. To assess the broader applicability of the design method, additional finite element analyses were carried out for slopes with varying geometrical and geotechnical properties. Finally, the paper discusses design considerations relevant to the application of flexible facings in combination with nailing.

KEYWORDS: flexible facing, flexible nail, slope stability analysis, field test, equilibrium method.

1 INTRODUCTION

1.1 *Flexible slope stabilization system*

The installation of a flexible facing in combination with systematic nailing has proven to be highly efficient for the stabilization of slopes at risk of failure in both rock and soil. Soil nails reinforce the natural soil and consequently enable the stabilization of the slope. The flexible facing commonly consists of steel wire mesh, which is connected to the nails by specific spike plates. The anchored mesh primarily serves to prevent local surficial instabilities in layers of soil or weathered rock. The mesh supports the soil between the nails and ensures the transmission of force between the slope surface and the nail head. Due to the pretensioning with a small force and the relatively small spacing of the soil nails, the steel wire mesh fits tightly on the slope surface, and even small deformations can activate the system.

1.2 *Flexible nail*

The flexible facing is typically installed in combination with systematic nailing, consisting of solid rebars or self-drilling anchors. As part of an innovation project, Geobrugg AG is collaborating with the Bern University of Applied Sciences on the development of a flexible nail for slope stabilization. The flexible nail consists of a high-strength stainless steel wire rope. Owing to its superior material quality, the flexible nail is lighter than comparable products, which not only makes it easier to handle but also reduces material consumption and carbon emissions.

1.3 *Design method*

The design of a flexible slope stabilization system is typically carried out using analytical methods. These methods are traditionally based on limit equilibrium calculations and assume either a slope-parallel planar slip surface or a polygonal slip surface (Blanco-Fernandez et al. (2011), Lambert & Bourrier (2024)). As systematic nailing remains the most labor-intensive aspect of installing a flexible slope stabilization system, optimal nail design is fundamental to the cost-efficiency of the system. This paper presents a new nail design method that is particularly suited for flexible nails.

1.4 *Validation*

A series of large-scale field tests were performed between 2012 and 2025 to investigate the structural behavior and failure mechanisms of a flexible slope stabilization system. The results of these tests are used to validate and optimize the design of the flexible slope stabilization system. While validation of the mesh design is already provided in several publications, e.g., Bucher et al. (2016), the present paper focuses on the validation of the nail design against experimental data from these large-scale field tests.

2 ANALYTICAL ANALYSIS

Flexible nails consisting of slender bars, cables, or ropes are predominantly subjected to normal forces when stabilizing slopes at risk of failure. In such cases, the shear load in the nail can be neglected (Hörtkorn, 2011). In contrast to existing design methods, as e.g. the RUVOLUM design approach (Cała et al., 2020), the proposed method treats the nails exclusively as tension members. Due to the high tensile capacity of flexible nails made of steel wire ropes or cable bolts, the method enables an efficient design by maximizing the mobilized tensile force within the flexible nail.

2.1 *Assumptions*

The design method for flexible nails is based on the following assumptions:

- Nails are subjected only to normal forces; shear forces are neglected due to the high flexibility of the nails.
- The slope is in a state of limit equilibrium.
- The slip surface is assumed to be slope-parallel.
- The Mohr–Coulomb failure criterion is applied along the slip surface; residual strength parameters are used.

2.2 *Slope of infinite length*

When the thickness of the unstable layer is small relative to the slope length, the analysis as an infinite slope may be appropriate. Analytical and numerical studies by Da Costa & Sagaseta (2010) suggest that when the ratio of the thickness of the shallow unstable layer to the height of the slope is less than 3%, the analysis as an infinite slope can be

considered adequate. In any case, the analysis as an infinite slope is conservative with respect to the design of the nails.

Figure 1 presents the situation of a supposed infinite slope, with parameters defined in Table 1. The solution to this problem is well known from the literature (e.g., Lambe & Whitman, 1969) and is presented hereafter in a consistent formulation for the sake of clarity.

The retaining force comprises the internal friction and cohesion mobilized at the base of the wedge, which are activated by the self-weight G and the nail force P. Additionally, a stabilizing slope-parallel force Z exerted by the mesh at the nail head is included in the stability analysis. This stabilizing force Z strongly depends on the stiffness of the mesh and the strength of the connection between the mesh and the nail head. Manufacturers provide recommended values for Z based on product-specific tests.

The internal friction force T and normal force N at the base of the wedge are related by the Mohr–Coulomb failure criterion:

$$T = N * \tan\varphi \qquad (1)$$

Solving the equilibrium of forces yields the nail force P required to stabilize the slope. A negative value of P indicates that no reinforcement is necessary.

$$P = \frac{G * [\sin\alpha - \cos\alpha \tan\varphi] - Z - c * a * b}{\cos(\alpha + \psi) + \sin(\alpha + \psi)\tan\varphi}\# \qquad (2)$$

The design of the nail requires comparing the calculated nail force P to the tensile capacity of the nail.

Table 1. Parameters for the nail design.

Symbol	Parameter
P	Nail force for slope stabilization
T_{nail}	Tension capacity of the nail
G	Weight of the wedge
Z	Slope parallel force exerted by the mesh
α	Slope inclination
ψ	Nail inclination to horizontal
φ	Angle of friction
c	Cohesion
a	Nail distance horizontal
b	Nail distance in line of slope
t	Unstable layer thickness

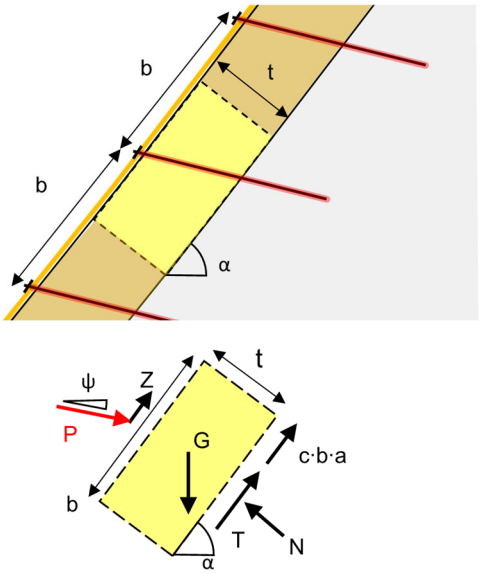

Figure 1. Slope of infinite length with free body force diagram.

2.3 *Slope of finite length*

As the ratio of the unstable layer thickness t to the slope length increases, the stabilizing effect of the toe of the slope becomes more significant. Consequently, accounting for the finite length of the slope can contribute to a more economical nail design.

The proposed failure mechanism consists of a polynomial slip surface and two wedges—an upper and a lower wedge. The dimensions of the wedges are defined by the geometrical properties of the slope (length L, inclination α), the thickness of the unstable layer t, and the inclination of the slip surface at the toe of the slope β (see Figure 2).

The stability analysis imposes equilibrium conditions on both the upper and lower wedge. The corresponding free-body force diagrams are shown at the bottom of Figure 2. To render the analysis statically determinate, a relationship between the internal contact forces X and Y acting between the wedges is assumed in the following form:

$$Y = X * \tan\delta\# \qquad (3)$$

The angle δ corresponds to the inclination of the internal contact surface relative to the wedge interface. Conservative values of the nail force may be obtained by setting $\delta = 0°$. The maximum possible value of δ is the largest inclination compatible with failure along the wedge interface; however, this typically leads to an underestimate of the required nail force. According to Morgenstern & Sangrey (1965), experience indicates that choosing δ between 10° and 15° usually yields reasonable results.

Solving the equilibrium of forces for both wedges provides the nail force P required to stabilize the slope.

$$P = f(\propto, \beta, \delta, \varphi, \psi, a, c, l_1, l_2, t, n_1, n_2, G_1, G_2, Z)\# \qquad (4)$$

The complete formulation for P is given in Equations (5), (6), (7) and (8) in the appendix to this paper. This formulation is clearly an extension of Equation (2). In the limit of very long slopes, where $l_1 >> l_2$, Equation (4) simplifies to Equation (2), used for infinite slope stability analysis.

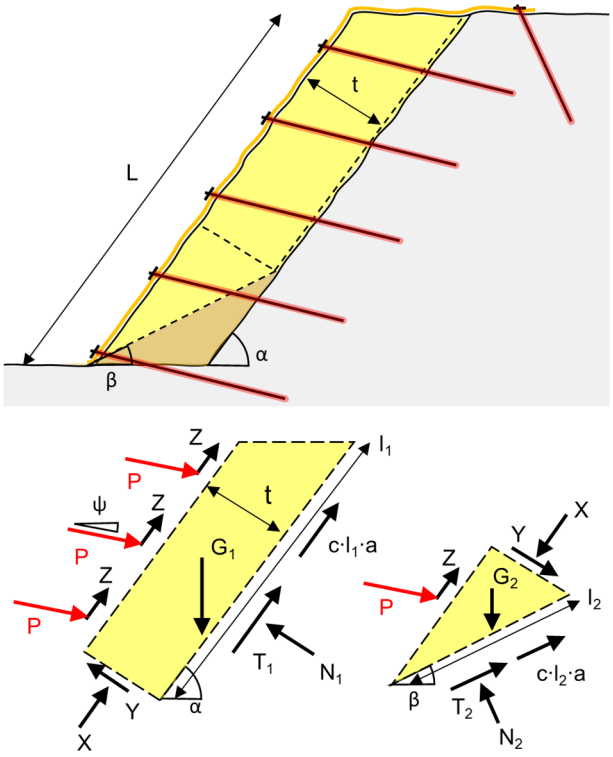

Figure 2. Slope of finite length with free body force diagram.

In addition to the parameters listed in Table 1, the stability analysis of a slope with finite length requires an additional set of parameters, which are summarized in Table 2. These additional parameters all depend on the inclination β of the slip surface at the toe of the slope. The inclination β must be varied between 0° and the maximum geometrically feasible value β_{max}. The value of β that corresponds to the maximum nail force P is decisive for design.

Table 2. Additional parameters for the nail design in a slope of finite length.

Symbol	Parameter
β	Inclination of the slip surface at the toe of the slope
G_1	Weight of the upper wedge
G_2	Weight of the lower wedge
n_1	Number of nail rows in the upper wedge
n_2	Number of nail rows in the lower wedge
l_1	Length of the slip surface along the upper wedge
l_2	Length of the slip surface along the lower wedge

3 LARGE SCALE FIELD TESTS

A total of 35 large-scale field tests were performed between 2012 and 2025 on flexible slope stabilization systems. By varying the distance between nails and the type of soil material, it was possible to analyze the structural behavior of different systems in detail.

3.1 *Test setup*

The test setup consisted of an artificial slope represented by a large-scale inclinable steel frame (12 × 10 × 1.2 m), which could be tilted on one side by a crane to simulate various slope angles (see Figure 3). The steel frame was incrementally inclined in 5° steps.

The nails used in the tests were threaded steel bars (ø 28 mm and 32 mm) and high-strength stainless steel wire ropes. The nails are encased in corrugated PVC tubes (ø 100 mm) and cemented in place to simulate realistic construction conditions. The nails were installed in regular patterns, perpendicular to the baseplate of the steel frame. All nails were rigidly fixed to the steel frame using steel foot plates.

The mesh cover was sewn to the upper and lower support ropes at the edges of the steel frame. Spike plates adapted to the mesh geometry were used to connect the mesh to the nails. The field test setup follows the European Assessment Document EAD 230025-00-0106 and is described in detail in Cała et al. (2020).

Figure 3. Test setup with the inclined steel frame.

3.2 *Soil material*

To analyze the behavior of the slope stabilization system under different soil conditions, two soil types with distinct strength parameters were selected, as summarized in Table 3. Both soils were classified according to the USCS Soil Classification System. The first soil was classified as poorly graded gravel (GP) and consisted of a mixture of 16 mm and 32 mm grains. The second soil was classified as poorly graded gravel with silt (GP-GM), with grain sizes ranging from 0 to 63 mm. The shear strength properties of the soils are derived from triaxial and direct shear tests (Derksen-Müller, 2013). In the large-scale field test, the soil was lightly compacted after being distributed across the box using a small excavator.

Table 3. Properties of the soil types used in the tests.

USCS	Friction angle φ [°]	Cohesion c [kPa]	Bulk density γ [kg/m³]
Poorly graded gravel GP	33	0	1750
Poorly graded gravel with silt GP-GM	38	0	1800

3.3 *Nail deformation*

The deformation of the mesh and nail heads was measured at each inclination step using a pulse laser scanner. A detailed analysis of mesh deformation in large-scale field tests is provided by Bucher et al. (2016). Figure 4 shows typical nail head deflection in the direction of the slope. Up to an inclination of 35° (tests with GP) and 45° (tests with GP-GM), no major deformations were observed. Significant mesh and nail deformation appeared at 40° (GP) and 50° (GP-GM), respectively. The large increase in deformation was associated with downward movement of the soil mass within the nail rows. The maximum nail deformation depended on nail spacing, mesh type, and soil type and typically ranged between 200 mm and 400 mm.

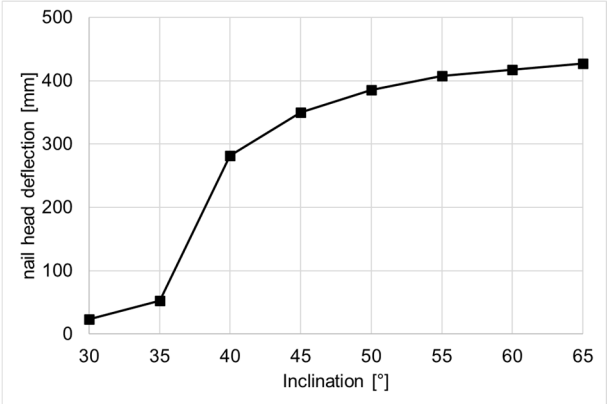

Figure 4. Deflection of the nail head in the line of the slope.

Some large-scale field tests were designed to investigate the performance limits of the slope stabilization system. Puncturing of the mesh at the nail head occurred once the load-bearing capacity of the mesh was exceeded. Figure 5 shows the test setup after failure. Notably, the nails themselves did not fail, although they experienced considerable deformation. In most cases, a plastic hinge formed at the base of the nail where it was fixed to the steel frame. This plastic hinge allowed the nail head to rotate in the direction of the slope. A similar behavior is plausible in real-world slopes where flexible nails are anchored in stable rock for surficial slope stabilization.

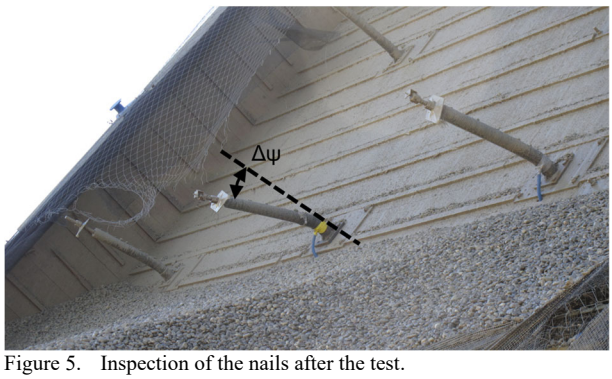

Figure 5. Inspection of the nails after the test.

In the proposed analytical design method, changes in nail inclination ψ significantly affect the calculated nail force (see Equation (2)). A reduction of the nail inclination to the horizontal generally results in a lower required nail force, which is favorable for design. However, accounting for nail inclination changes due to soil deformation is a controversial issue (Michalowski, 1998). A conservative approach considers the undeformed nail orientation in design calculations.

3.4 *Nail forces*

The relevant nails in the lower and central parts of the steel frame were instrumented to determine the nail forces. Strain gauges were installed on four sides of the solid rebars to measure not only the normal forces but also the bending moments in the nails. Measurements were taken in two sections along each rebar: one near the bottom of the steel frame and the other near the nail head. The forces in the nails made of wire rope were measured using load cells (Sisgeo, 750 kN) installed at both the nail head and the bottom of the steel frame (see Figure 6).

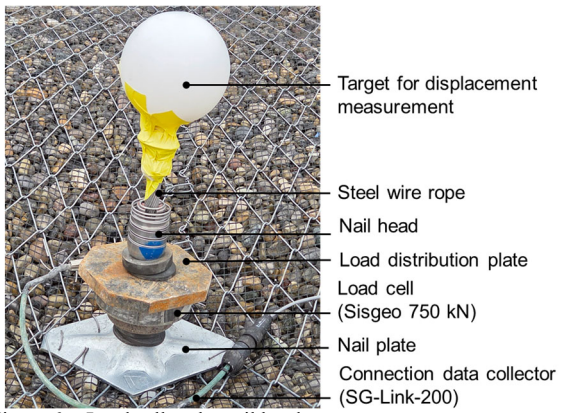

Figure 6. Load cell at the nail head.

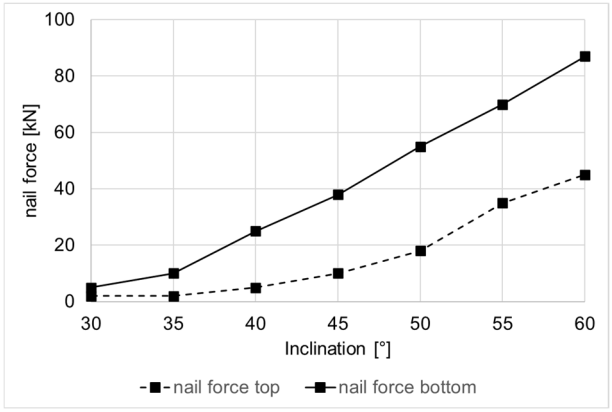

Figure 7. Nail force at the top and the bottom of the nail measured in field test 21.

Figure 7 shows the measured nail force for one nail in Test 21 at the measurement section near the nail head and near the bottom of the steel frame. The nail force was consistently higher near the bottom of the nail, close to the expected slip surface, and decreased toward the nail head due to skin friction. The skin friction of the nail was up to 60 kN/m, calculated based on the difference in nail force between the two measurement sections which are approximately 0.7 m apart.

3.5 *Validation of the design method*

To validate the design method proposed in Chapter 2, the forces measured in the large-scale field tests were compared with the analytically derived nail forces calculated according to Equation (5). The nails used in the tests included threaded steel bars and high-strength stainless steel wire ropes, both of which exhibited flexible behavior due to their relatively low area moment of inertia and the formation of a plastic hinge at the base (see Chapter 3.3). Table 4 summarizes the characteristics of the test setups used in the validation.

Table 4. Characterization of the test setups.

Test nr.	Nail spacing [m]	Nail type	Soil type
18	3.0 x 3.0	steel bar ø 28 mm	GP-GM
21	3.0 x 3.0	steel bar ø 28 mm	GP
27	2.5 x 2.5	steel bar ø 28 mm	GP-GM
33	2.0 x 2.0	steel bar ø 28 mm	GP-GM
37	3.0 x 3.0	steel wire rope	GP

The comparison of the analytically calculated nail forces with the measured values is presented in Figure 8. The figure shows the nail with the highest measured force in each respective test. In Test 33, the nails were pretensioned to 20 kN and therefore exhibited measurable force even at very low inclinations.

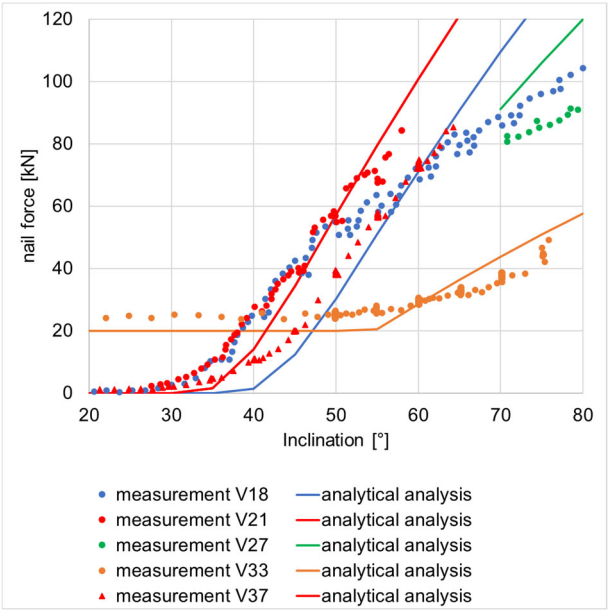

Figure 8. Comparison of the nail forces according to the measurement and the analytical design method.

The calculated and measured nail forces show good agreement. Particularly for a common nail pattern with a spacing of 3.0 m multiple tests were conducted. The tests with a comparable setup show similar nail forces indicating good reproducibility. At high inclinations of the steel frame, the analytical method slightly overestimates the measured forces, likely due to conservative parameter choices used in the validation (see Table 5).

Table 5. Parameters used for the validation of the design method.

Parameter		Test 18	Test 21	Test 27	Test 33
α	[°]	0 – 84	0 – 57	0 – 80	0 – 75
ψ	[°]	90-α	90-α	90-α	90-α
γ	[kN/m³]	18.0	17.5	18.0	18.0
φ	[°]	38	33	38	38
c	[kPa]	0	0	0	0
a	[m]	3.0	3.0	2.5	2.0
b	[m]	3.0	3.0	2.5	2.0
t	[m]	1.2	1.2	1.2	1.2
L	[m]	10.0	10.0	10.0	10.0
n	[-]	3	3	3	5
δ	[°]	0*	0*	0*	0*
Z	[kN]	0*	0*	0*	0*

* The parameters are chosen conservatively due to the limited reliability of their determination in the tests.

4 NUMERICAL ANALYSIS

To assess the broader applicability of the proposed design method, additional finite element analyses with PLAXIS 2D (Brinkgreve & Vermeer, 1998) were conducted for slopes with varying properties. Accordingly, the nail forces obtained from the finite element simulations were compared with the analytically calculated nail forces.

4.1 *Model geometry*

The setup of the finite element model and the corresponding geometrical properties are illustrated in Figure 9. The analysis focuses on potential instabilities within a soil layer of 1.50 m thickness. Failure mechanisms involving deeper sliding surfaces are excluded by assuming a competent rock mass underlying the soil. The slope length L varies between 15 m and 30 m, and the slope inclination varies between 50° and 70°.

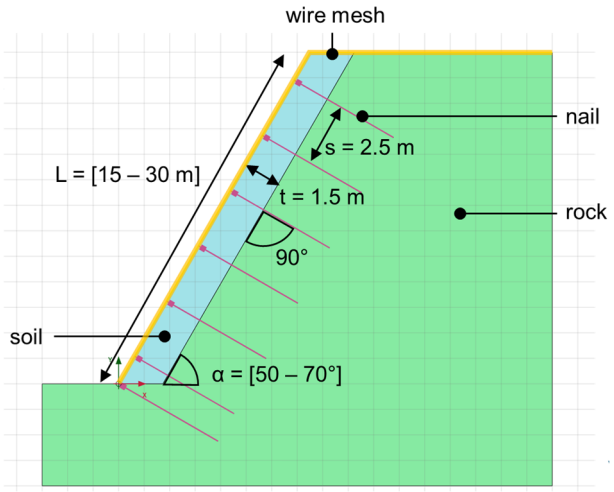

Figure 9. Setup of the finite element model.

4.2 *Mechanical properties*

The soil is modeled with an elastic, perfectly plastic constitutive behavior and a Mohr–Coulomb failure criterion. The corresponding mechanical properties are provided in Table 6.

Table 6. Mechanical properties of the soil.

Parameter			Description
γ	[kN/m³]	18.0	Unit weight
E	[kN/m²]	30e3	Young's modulus
ν	[-]	0.2	Poisson's ratio
φ	[°]	38	Friction angle
c	[kN/m²]	1*	Cohesion

* A minimum cohesion is considered for numerical stability.

The underlying rock is also modeled as an elastic, perfectly plastic material with a Mohr–Coulomb failure surface. Its mechanical properties correspond to those of a typical sedimentary rock and are summarized in Table 7. The relatively high cohesion prevents failure within the rock mass.

Table 7. Mechanical properties of the rock.

Parameter			Description
γ	[kN/m³]	24.0	Unit weight
E	[kN/m²]	1.5e6	Young's modulus
ν	[-]	0.25	Poisson's ratio
φ	[°]	40	Friction angle
c	[kN/m²]	250	Cohesion

The nail is represented by an elastic beam element. Its properties correspond to a flexible nail made of a steel wire rope and are listed in Table 8.

Table 8. Mechanical properties of the nail.

Parameter			Description
γ	[kN/m³]	24.0	Unit weight
s	[m]	2.5	Spacing
E	[kN/m²]	200e6	Young's modulus
A	[mm²]	273	Cross section area
I	[mm⁴]	200	Second moment of inertia
T_{skin}	[kN/m]	50	Skin resistance of the nail

The mesh is modeled as an elastic membrane element. Its mechanical properties correspond to the TECCO product type (Cała et al., 2020) and are provided in Table 9.

Table 9. Mechanical properties of the mesh.

Parameter			Description
γ	[kN/m²]	0	Unit weight, neglectable
EA_1	[kN/m]	3000	Normal stiffness in slope direction
EA_2	[kN/m]	300	Normal stiffness parallel to slope

4.3 *Nail forces*

For each calculation case, the nail forces required to stabilize the slope were evaluated. The maximum normal forces obtained from the finite element analysis are shown as solid lines in Figure 10. The results indicate that the longer and steeper the slope, the greater the normal force required in the nail. The maximum nail force occurred near the slip surface and decreased toward the nail head. Nails located near the toe and crest of the slope exhibited slightly lower normal forces than those in the middle. Due to the high flexibility of the nail, the bending moment and shear force were negligible.

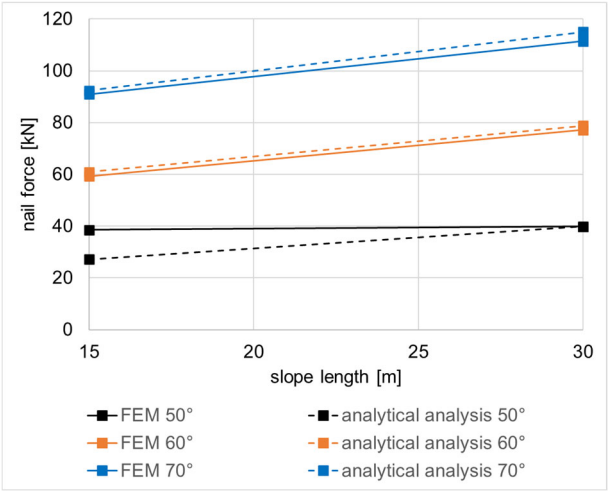

Figure 10. Normal force in the nail for different slope lengths and slope inclination according to the numerical and analytical analysis.

The slip surface in the finite element model manifests as a zone of pronounced deviatoric strain. It generally follows the bottom

of the surficial soil layer and exits at the toe of the slope, corresponding well to the block geometry assumed in the analytical model (see Figure 2).

Figure 10 also shows with dotted lines the nail forces calculated using the analytical design method presented in Chapter 2. A reasonable agreement is observed between the analytical and finite element results. While both methods yield comparable outcomes, the analytical approach is clearly the simpler and more efficient method for calculating nail forces.

5 CONCLUSIONS

A novel analytical design method particularly suited for flexible nails used in surficial slope stabilization is proposed. Distinct formulations are provided for the analysis of very high slopes, assumed to be infinitely long, and for slopes of limited length. In contrast to existing design methods, the proposed approach treats the nails exclusively as tension members. The validity of the design method and its underlying assumption for flexible nails (e.g. slender bars or steel wire ropes) is supported by the nail force measurements of unique large-scale field tests. The comparison between the maximum measured nail forces in the field tests and the analytically calculated values shows good agreement.

The tests were thoroughly analyzed with respect to the behavior of the nails and the mesh. It was found that the maximum force in the nail occurs near the intersection of the nail with the presumed slip surface along the baseplate of the steel frame. The nail force decreases toward the nail head due to skin friction between the grouted body and the surrounding soil. Several large-scale field tests were conducted to investigate the performance limits of the slope stabilization system. System failure occurred at the nail head due to puncturing of the nail head through the mesh. The nails themselves did not fail in any of the tests, although they exhibited significant deformation.

The broader applicability of the proposed design method was further assessed through additional finite element analyses performed using the commercial software PLAXIS. These analyses focused on instabilities within a 1.50 m thick soil layer. The comparison of the maximum nail force and the slip surface obtained from the finite element analysis demonstrates good agreement with the analytically calculated nail force and the assumed failure surface. Consequently, the proposed analytical method provides a valid and straightforward approach for designing nails in surficial slope stabilization systems that employ flexible facings.

6 ACKNOWLEDGMENTS

The work presented is part of the Innosuisse research project “Entwicklung einer gesamtheitlichen flexiblen Böschungsstabilisierung mit neuem flexiblem Seilnagel”. The authors express their sincere gratitude to the Swiss Innovation Agency for its support.

7 REFERENCES

Blanco-Fernandez, E., Castro-Fresno, D., Del Coz Díaz, J.J. and Lopez-Quijada, L. 2011. Flexible systems anchored to the ground for slope stabilisation: Critical review of existing design methods. *Engineering Geology*, Volume 122 (Issues 3-4), 129-145.

Brinkgreve, R.B.J. and Vermeer, P.A. 1998. *Plaxis 2D V7*. Manual. Rotterdam: A.A. Balkema.

Bucher, R., Wendeler, C. and Baraniak, P. 2016. New results of large-scale testing of high-tensile steel meshes and soil nails for slope stabilisation and validation of modelling software. Australian Center for Geomechanics, *First Asia Pacific Slope Stability in Mining Conference.* Perth (2016).

Cała, M., Flum, D., Roduner, A., Rüegger, R and Wartmann, S. 2020. *TECCO® Slope Stabilization System and RUVOLUM® Dimensioning Method*. Cracow: AGH University of Science & Technology.

Da Costa, A. and E., Sagaseta C. 2010. Analysis of shallow instabilities in soil slopes reinforced with nailed steel wire meshes. *Engineering Geology*, Volume 113 (Issues 1-4), 53-61.

Derksen-Müller, S. 2013. Analysis of soil properties of material used in large scale field tests on flexible facing systems for slope stabilization. Zürich: Eidgenössische Technische Hochschule.

EOTA, 2016. *EAD 230025-00-0106, Flexible Facing Systems for Slope Stabilization and Rock Protection*. EOTA.

Hörtkorn, F. 2011. *Wirksamkeit von flexiblen stabförmigen Elementen bei Böschungsstabilisierungen*. Cracow: AGH University of Science & Technology. Kassel: Schriftenreihe Geotechnik Universität Kassel (Heft 24).

Lambert, S. and Bourrier, F. 2024. Flexible Facing Systems for Surficial Slope Stabilisation: A Literature Review. *Geotechnical and Geological Engineering*, Volume 42, 5425-5446.

Lambe, T.W. and Whitman, R.V. 1969. *Soil Mechanics*. New York: John Wiley.

Michalowski, R.L. 1998. Limit analysis in stability calculations of reinforced soil structures. Geotextiles and Geomembranes, Volume 16 (Issues 6), 311-331.

Morgenstern, N.R. and Sangrey, D.A. 1978. *Landslides: Analysis and Control, Chapter 7: Methods of Stability Analysis*. Washington DC: Transportation Research Board.

APPENDIX

Equations (5), (6), (7) and (8) enable to calculate the nail force in a slope with finite length (see chapter 2.3).

$$P = \frac{\omega * \Lambda * \{G_1[\sin\alpha - \cos\alpha\tan\varphi] - n_1 * Z - C_1\} + G_2[\sin\beta - \cos\beta\tan\varphi] - n_2 * Z * [\cos(\alpha-\beta) - \sin(\alpha-\beta)\tan\varphi] - C_2}{\omega * \Lambda * n_1 * [\cos(\alpha+\psi) + \sin(\alpha+\psi)\tan\varphi] + n_2 * [\sin(\beta+\psi)\tan\varphi + \cos(\beta+\psi)]} \quad (5)$$

$$C_i = c * a * l_i \quad (6)$$

$$\omega = \frac{1}{1 - \tan\delta\tan\varphi}\# \quad (7)$$

$$\Lambda = \cos(\alpha-\beta)\{1 - \tan\delta * \tan\varphi\} - \sin(\alpha-\beta)\{\tan\delta + \tan\varphi\}\# \quad (8)$$